Journal of Porphyrins and Phthalocyanines
J. Porphyrins Phthalocyanines 2014; **18**: 771–777
DOI: 10.1142/S1088424614500552

Published at http://www.worldscinet.com/jpp/

Self-assembled phthalocyanine derivatives on highly ordered pyrolytic graphite

S. Gokhan Colak[a] and Mine Ince*[a,b◊]

[a] *Advanced Technology Research & Application Center, Mersin University, Ciftlikkoy Campus, TR-33343 Mersin, Turkey*
[b] *Department of Energy Systems Engineering, Mersin University, Tarsus Faculty of Technology, TR-33480 Mersin, Turkey*

Dedicated to Professor Nagao Kobayashi on the occasion of his 65th birthday

Received 13 July 2014
Accepted 18 August 2014

ABSTRACT: A novel unsymmetrically substituted hydroxy-functionalized Zn(II) phthalocyanine (Pc) **1**, bearing long aliphatic chains, namely, dodecyloxy units, has been designed and synthesized to investigate the influence of the terminal hydroxyl group on the formation of self-assembled nanostructures. The symmetric derivative, octadodecyloxy-Zn(II)Pc (**2**) has been also synthesized and used as reference compound for comparison purposes. The supramolecular organization of the Pcs has been carried out by spin-coating on a highly ordered pyrolytic graphite (HOPG) surface and has been investigated by atomic force microscopy (AFM) and scanning electron microscopy (STM). AFM and STM studies showed that unsymmetrically substituted hydroxy-functionalized Zn(II)Pc **1** gives rise to the formation of wire-like structures in different lengths from nanometer to micrometer scales, whereas in the case of the symmetrical Zn(II)Pc **2** the formation of the wires on HOPG was less pronounced.

KEYWORDS: phthalocyanines, self-assembly nanostructures, molecular wires, supramolecular electronics.

INTRODUCTION

The construction of self-assembled nanostructures by means of supramolecular interactions such as electrostatic, hydrogen bonding, π–π stacking, and coordinative bonding (metal–ligand) has received much attention in the field of optoelectronics since the spontaneous self-organization of the molecules into highly ordered supramolecular structures, with controlled dimensions and size is a key point for the development of efficient devices [1]. Generally, the performance of such optoelectronic devices is dominated by molecule-to-molecule and molecule-to-surface supramolecular interactions [2]. In particular, Pcs, among the organic dyes, are one of the most extensively studied functional molecular components for molecular photovoltaics, optoelectronic applications, and in the study of photoinduced electron transfer processes due to their suitable photophysical properties, self-organization ability, and remarkable chemical and thermal stability [3]. Pcs are macroheterocyclic compounds having 18-π electron system and are synthetic analogs of the naturally occurring porphyrins. The electronic absorption spectrum of Pcs shows two main bands, the Q-band and the Soret or B-band. The Q-band, associated to π–π* HOMO–LUMO transition, is usually found in the region of 620–700 nm and is responsible for the deep green or blue color of these compounds. These bands can be easily tuned by the careful choice of the metal atom in the macrocycles cavity and by placing adequate substituents at the macrocycles peripheral and axial positions [4]. The unique physicochemical properties of Pcs have prompted the incorporation of these macrocycles in widespread applications in materials science. Up to date, a wide range of supramolecular interactions have been used in the

---

[◊] SPP full member in good standing

*Correspondence to: Mine Ince, email: mine.ince@mersin.edu.tr, tel: +90 324-361-0001-4980, fax: +90 324-361-0153 fabrication of Pc-based nanoscale functional systems to improve their photophysical and (opto)electronic properties on surfaces and in liquid crystalline phases as a result of interactions between the dyes and/or substrate [5]. For instance, Pcs bearing flexible peripheral substituents represent typical examples of discotic mesogens in which the molecules form efficient columnar stacks and some of them produce high-charge carrier mobility, due to intense π–π interactions between the macrocycle cores [6]. Concerning the "bottom-up" approach for the construction of Pcs based systems on surfaces, the formation of two-dimensional self-assembled monodispersed molecules on HOPG has been achieved by using the single-molecule magnet alkoxy-substituted bis(phthalocyaninato)terbium(III) [7]. Similarly, the highly ordered self-assembled structure of octa-alkoxyl substituted Pc on the HOPG surface has been also reported [8]. The enhanced interactions of Pc molecules with the substrate as the result of the presence of octa-alkoxy groups allows the formation of quadratic lattices which could be used as templates for trapping individual molecules. As an interesting example, Torres and co-workers reported a covalently linked Pc-fullerene conjugate which is able to form highly organized supramolecular films and fibers on HOPG [9].

In this context, the present paper is focused on the synthesis of a novel unsymmetrically substituted hydroxy-functionalized Zn(II)Pc (**1**) (Chart 1) which bears long aliphatic dodecyloxy chains for the construction of properly ordered Pc-based nanostructures on a HOPG surface. Moreover, a symmetric derivative, octadodecyloxyZn(II)Pc (**2**) was synthesized and used as reference compound. Supramolecular organization of the Pcs on HOPG was examined by AFM and STM in order to investigate the influence of terminal hydroxyl groups on the self-assembly features of the Pcs. The self-organizational differences between the unsymmetrical Zn(II)Pc **1** and the structurally related symmetric Zn(II)Pc **2** has been also discussed.

EXPERIMENTAL

General

All chemicals were purchased from Aldrich and used without further purification. Column chromatography was carried out on silica gel Merck-60 (230–400 mesh, 60 Å), and TLC was carried out on aluminium sheets percolated with silica gel 60 F254 (E. Merck). The IR spectra were performed with Perkin–Elmer, FT-IR/MIR-FIR (ATR, Attenuated total reflectance) spectrophotometer. MALDI TOF-MS spectra were determined on a BRUKER Microflex LT. NMR spectra were recorded with a Bruker AC-400 instrument. UV-vis spectra were recorded with a Analytic JENA S 600 UV-vis spectrophotometer. Atomic Force Microscopy (AFM) and Scanning Tunneling Microscopy (STM) studies were carried out using a Park System XE-100 SPM instrument under ambient conditions using a commercial scanning probe microscope. The AFM topographic images were analyzed using Park Systems XEI software. The samples of Pcs in an organic solvent were spin-coated onto HOPG surface and measured under ambient conditions.

Synthesis

Synthesis of Zn(II)Pc derivatives 1 and 2. A mixture of 4,5-bis(dodecyloxy)phthalonitrile (**3**) (620 mg, 1.25 mmol), 4-[(4-hydroxymethyl)phenyl-ethynyl]phthalonitrile (**4**) (80 mg, 0.31 mmol) and $Zn(OAc)_2$ (90 mg, 0.49 mmol) in DMAE (6 mL) was heated at reflux for 24 h with stirring under argon atmosphere. After cooling to room temperature, the solvent was removed and the residue was washed with a $MeOH/H_2O$ (5:1) mixture. The crude product was purified by column chromatography on silica gel (toluene/THF, 12:1). The symmetric Zn(II)Pc **2** was eluted first, obtaining 210 mg (0.10 mmol, 32% yield), followed by Zn(II)Pc **1**, 155 mg (0.08 mmol).

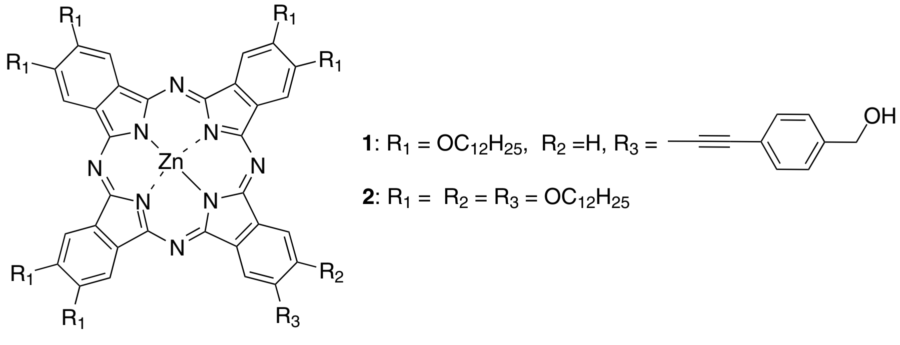

Chart 1. Molecular structures of Zn(II)Pcs **1** and **2**

Zinc(II) 9,10,16,17,23,24-hexadodecyloxy-2-[2´-(4´-(hydroxymethyl)-phenyl)ethynyl] phthalocyaninato(2-)-N^{29}, N^{30}, N^{31}, N^{32} (1). Yield 155 mg (27%). ^{1}H NMR (THF-d_8, 400 MHz): δ, ppm 9.7 (s, 2H; Ar-H), 9.3 (s, 1H; Ar-H), 9.06 (d, 1H, *J* = 8 Hz, Ar-H), 8.6 (s, 1H; Ar-H), 8.5 (s, 1H; Ar-H), 8.5–8.4 (m, 2H; Ar-H), 8.1 (d, *J* = 8 Hz, 1H, Ar-H), 7.82 (d, *J* = 8 Hz, 2H, Ar-H), 7.54 (d, *J* = 8 Hz, 2H, Ar-H), 4.73 (d, *J* = 4 Hz, 2H, Ar-H), 4.6–4.4 (m, 12H; Alkyl-H), 2.2–2.1 (m, 12H; Alkyl-H), 1.9–1.7 (m, 12H; Alkyl-H), 1.3–1.2 (m, 96 H, Alkyl-H) 0.9–0.8 (m, 18H; Alkyl-H). IR (ATR): ν, cm^{-1} 2955, 2853, 1763, 1712, 1602, 1485, 1384, 1281, 1045, 881, 744. UV-vis (THF): λ_{max}, nm (log ε) 687 (4.96), 672 (4.91), 611 (4.3), 356 (4.76). MS (MALDI, dithranol): *m/z* 1813.2 $[M]^+$.

Zinc(II) 2,3,9,10,16,17,23,24-octakis(dodecyloxy)-phthalocyaninato(2-)-N^{29}, N^{30}, N^{31}, N^{32} (2). Yield 210 mg (32%). ^{1}H NMR (THF-d_8, 400 MHz): δ, ppm 8.8 (s, 8H; Ar-H), 4.6–4.5 (m, 16H; Alkyl-H), 2.1–2.0 (m, 16H; Alkyl-H), 1.4–1.2 (m, 144H; Alkyl-H), 0.9–0.8 (m, 24H; Alkyl-H). IR (ATR): ν, cm^{-1} 2956, 2918, 2849, 1730, 1606, 1495, 1456, 1381, 1277, 1201, 1094, 1072, 853, 798. UV-vis (THF): λ_{max}, nm (log ε) 672 (5.05), 646 (4.31), 607 (4.30), 355 (4.68). MS (MALDI, dithranol): m/z 2052.4 $[M]^+$.

RESULTS AND DISCUSSION

Synthesis

The hydroxy-functionalized Zn(II)Pc **1** was synthesized following the routes depicted in Scheme 1. The 4,5-bis(dodecyloxy)phthalonitrile (**3**) [10], and 4-[(4-hydroxymethyl)phenyl-ethynyl]phthalonitrile (**4**) [6c] were successfully synthesized according to literature procedures. It is known that the synthesis of unsymmetrically substituted Pcs consisting of three identical isoindole subunits and a fourth different one (A_3B) by statistical cross-condensation of two-differently substituted phthalonitrile precursors is a relatively well-known process. The approach relying on the statistical reaction of two different phthalonitrile precursors A and B in a ratio of 3:1 to 9:1 appears to be the most commonly applied. However, this method produces a mixture of all the possible macrocycles (A_4, A_3B, A_2B_2, AB_3, etc.), and the isolation of desired Pcs from the mixture usually requires extensive chromatographic purification. In this regard, the steric effect of the substituents and ratio and reactivity of the phthalonitrile precursors have to be taken into account to facilitate the separation and to increase the yield of the desired unsymmetric compound. Thus, the condensation reaction of 4,5-bis(dodecyloxy) phthalonitrile (**3**) (four equivalents) with the corresponding hydroxy-functionalized phthalonitrile **4** (one equivalent) in the presence of zinc(II) acetate generates a statistical mixture of compounds in which the major components are symmetrically substituted Pc **2**, followed by unsymmetrically substituted hydroxy-functionalized Pc **1**. Purification by silica gel column chromatography gave rise to Zn(II)Pc **1** in 27% and Zn(II)Pc **2** in 32% yield.

Due to the presence of the long alkyl chains, both Pc compounds are highly soluble in common organic solvents such as CH_2Cl_2, $CHCl_3$, toluene, and THF. The structure and purity of both compounds was checked by ^{1}H NMR, IR, UV-vis and MALDI-TOF spectroscopy. Generally, the ^{1}H NMR spectra of Zn(II)Pc derivatives are poorly resolved in non-coordinating solvents like $CHCl_3$ due to aggregation. However, Zn(II)Pcs **1** and **2** gave well-resolved and informative ^{1}H NMR spectra in a coordinating solvent such as THF-d_8 where each proton of the Pc macrocycle was easily assigned with signals between 7.8 and 9.6 ppm. Figure 1 shows the ^{1}H NMR spectrum of Zn(II)Pc **1** as an example.

UV-visible spectroscopy

It is well-established that the electronic absorption spectra of Pcs strongly depends on the solvent polarity [4]. For example, in non-coordinating solvents such as toluene or $CHCl_3$, often, the absorption corresponding to

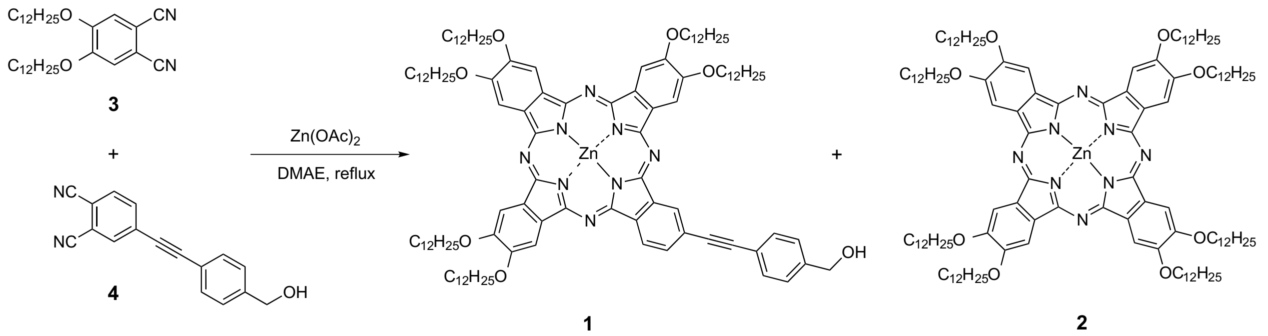

Scheme 1. Synthetic route to symmetrical and hydroxy-functionalized Zn(II)Pcs **1** and **2**

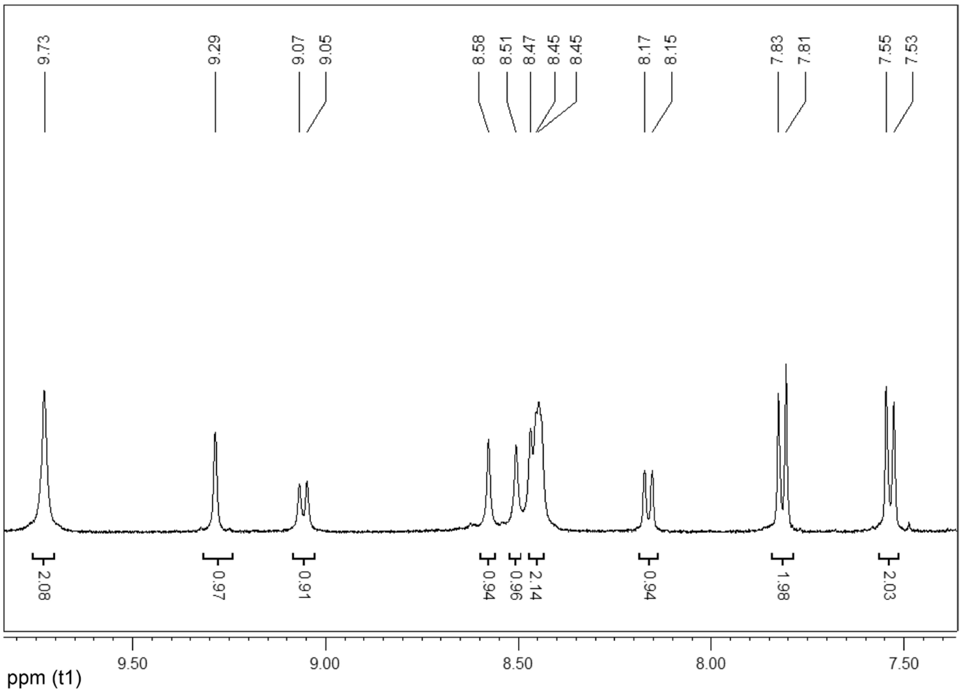

Fig. 1. ^{1}H NMR spectrum of Zn(II)Pc **1** in THF-d$_8$

the Q-band observed as broad band in the range of 600–700 nm due to intermolecular π–π interaction between two Pc macrocycles. However, this interaction can be broken up in coordinating solvents such as THF which provides axial coordination to the zinc metal center that avoids macrocycle aggregation. UV-vis absorption spectra of Zn(II)Pcs **1** and **2** in toluene are depicted in Figs 2 and 3. For comparison purposes, UV-vis experiments were also carried out in a polar and coordinating solvent such as THF. ZnPc(II) **1** exhibits a split Q-band with maximum at 690 nm in toluene. The absorption spectrum of Zn(II)Pcs **1** in THF is very similar to the one in toluene with absorption maximum at 687 nm. This result suggests that Zn(II)Pc **1** does not display any important aggregation features in toluene.

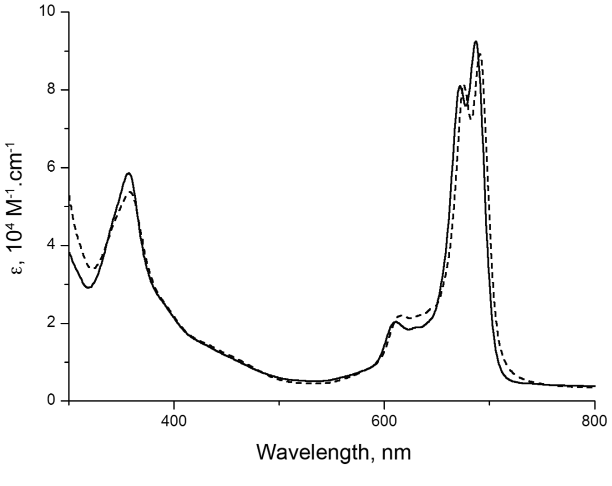

Fig. 2. UV-vis absorption spectra of Zn(II)Pcs **1** in THF (solid line) and toluene (dashed line) (~1 × 10^{-5} M)

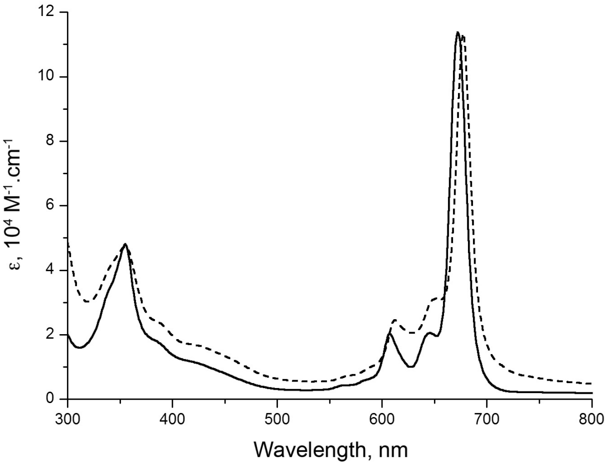

Fig. 3. UV-vis absorption spectra of Zn(II)Pc **2** in THF (solid line) and toluene (dashed line) (~1 × 10^{-5} M)

The UV-vis absorption spectrum of symmetric Zn(II) Pc **2** in THF exhibits sharp Q-band with an absorption maximum located at 672 nm corresponding to the monomeric species (Fig. 3). When the solvent changes from THF to toluene, similar absorption feature is observed. Nevertheless, a small red shift of the Q-band (*ca.* 5 nm) was observed in toluene. On the other hand, in comparison with symmetric Zn(II)Pc derivative **2**,

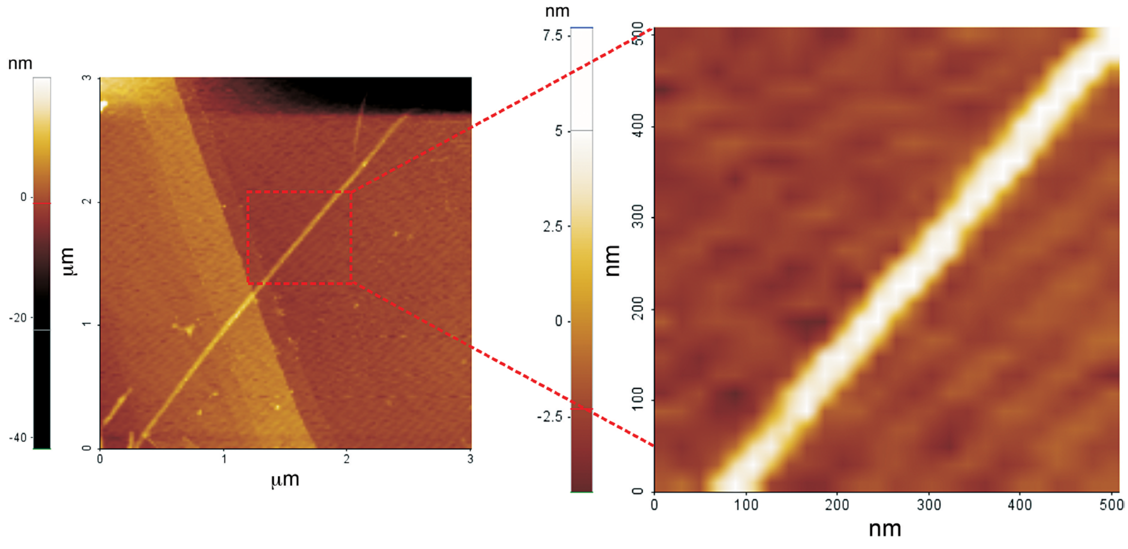

(a) (b)

Fig. 4. (a) Tapping-mode AFM images of Zn(II)Pc **1** on HOPG. (b) AFM image of a magnified area of (a)

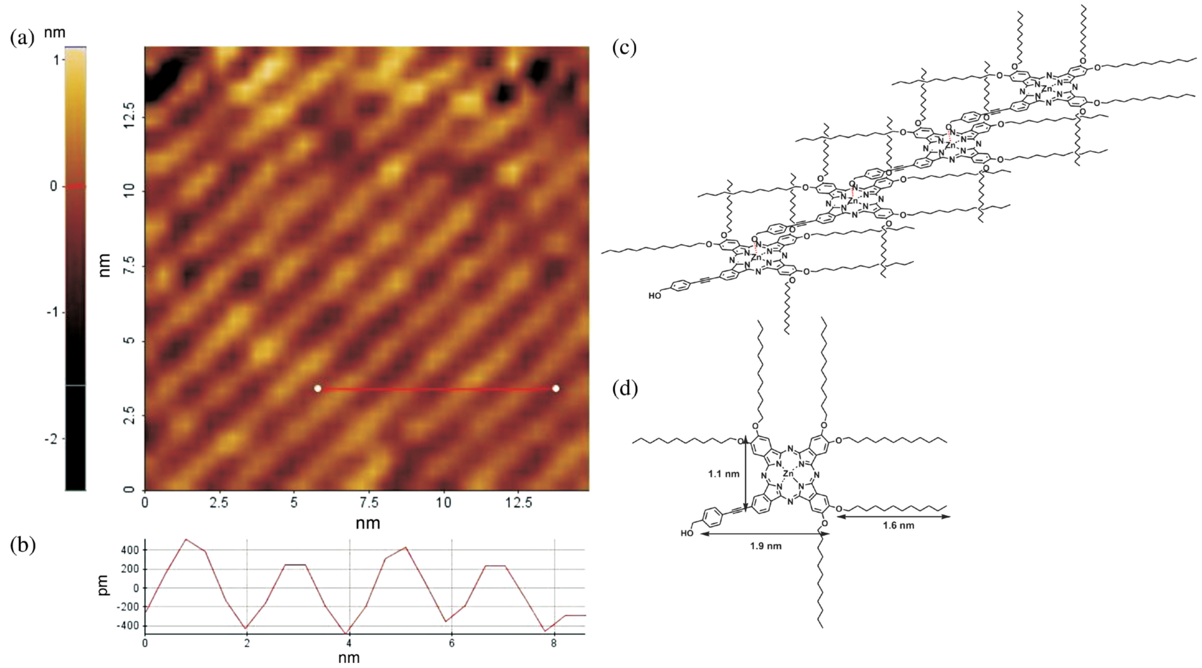

Fig. 5. (a) High-resolution STM analysis of a Zn(II)Pc **1** molecular wire on HOPG. (b) The length and height profile along the red line in (a) (line scan). (c) Schematic representation of the possible organization of Zn(II)Pc **1** on HOPG surface. (d) Estimated molecular dimensions of Zn(II)Pc **1**: macrocyclic core is to be 1.1 nm, Pc core with terminal hydroxyl group is to be 1.9 nm and the length of dodecyloxy chain is 1.6 nm

the Q-bands of Zn(II)Pc **1** undergo a red shifting, *i.e.* 15 nm, with concomitant splitting of the Q-band which symmetrically substituted Zn(II)Pc **2** does not exhibit.

Organization of Zn(II)Pcs on a HOPG surface

Supramolecular organization of unsymmetrical Zn(II) Pc **1** and symmetric Zn(II)Pc **2** on HOPG surface was investigated by AFM and STM. A freshly prepared solution of Zn(II)Pcs in toluene (c ~ 10^{-5} M) was deposited by a spin-coating technique on HOPG and allowed to evaporate. AFM studies of Zn(II)Pc **1** on HOPG surfaces revealed the formation of wire-like structures in different lengths from nanometer to micrometer scales (Fig. 4a). Detailed AFM investigations confirmed that Zn(II)Pc **1** self-assembles into well-ordered π-stacks on a HOPG

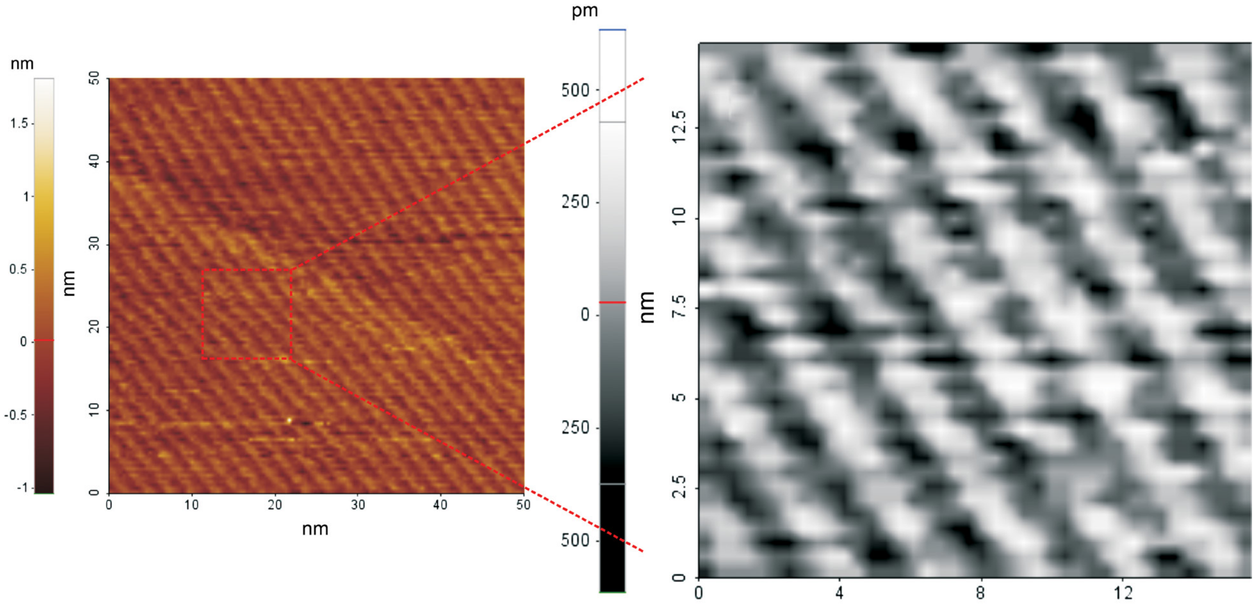

(a) (b)

Fig. 6. (a) High-resolution STM analysis of Zn(II)Pc **2** on HOPG. (b) Magnified STM image of the selected area

surface (Fig. 4b). The lengths of the wires on the surface are in the range of 3–10 µm, and the diameter of the wires are between 40–60 nm.

To gain further insight into the self-organization of Zn(II)Pc **1** on HOPG surface, STM studies were performed. High-resolution STM analysis of a Zn(II)Pc **1** molecular wire on HOPG is shown in Fig. 5. The STM image is given in Fig. 5 was obtained by focusing on the molecular wire structure determined by AFM measurement (Fig. 4). STM studies reveal the formation of single stacks of parallel-oriented ZnPc **1**, in which the Pc molecules are tilted with respect to the surface (Fig. 5b). This nanowire arrangement on the surface could result from the intermolecular π–π interactions of macrocyclic core as well as Zn—OH interactions between the central metal of Zn(II)Pc **1** and the terminal oxygen which hindering the formation of a closed-packing array on the HOPG.

A closer look at the STM images indicates that single stacks of Pcs molecules are organized in ordered parallel lines, in which the alkyl chains of one stack are all arranged in the same direction. The periodicity of organization of single molecule into nanowire is about 2 nm which shows a good agreement with the dimension of the molecule which is shown in Fig. 5c. In this context, the larger molecular wire structures (diameter 40–60 nm) observed by AFM studies (Fig. 4) are assumed to be composed of many single wires with an about 2 nm diameter aligned parallel to each other.

On the other hand, under similar conditions, the absorption of symmetric Zn(II)Pc **2** on the HOPG surface leads the formation of closed-packed array revealed by STM (Fig. 6). This could be explained by the fact that the strong π–π interactions between Pc molecules are more pronounced in the case of symmetric Pc compounds. Although the molecular pattern of symmetric Pc **2** seems to be similar to that of unsymmetrical derivative, it should be noted that, in the case of Zn(II)Pc **1** molecular patterns were obtained from the nanowire which is shown in Fig. 4.

Within the unsymmetrical Pc molecules, the long dodecyl chains are hydrophobic and the remaining part, the –OH moiety is relatively hydrophilic. On the hydrophobic HOPG surface, wire self-aggregates were only observed with unsymmetric Pc **1**. However, organization of **1** was not detected on hydrophilic surfaces such as mica and quartz. Furthermore, amorphous and irregular structures were observed during studies carried on hydrophilic surfaces with both unsymmetric and symmetric Pcs. This result shows that hydrophobic surfaces play an important role in wire formations. Thus, molecules surrounded with long –OR moieties are stabilized on the hydrophobic surface by the assistance of appropriate interaction of the long chains in the main core [11].

SUMMARY AND CONCLUSIONS

A novel unsymmetrically substituted hydroxy-functionalized Pc **1** bearing long aliphatic dodecyloxy chains has been synthesized as the building block for the construction of multipurpose materials for potential optoelectronic applications. UV-vis absorption studies showed that both unsymmetrically and symmetrically substituted Zn(II)Pcs derivatives **1** and **2** respectively exhibited monomeric forms in toluene. AFM studies of unsymmetrical substituted Pcs **1** on the graphitic surface revealed the formation of wire-like structures in different lengths from nanometer to micrometer scale. On the other hand, symmetrically substituted Zn(II)Pc **2** exhibited the formation of the closed-packed array rather than wires on HOPG surface. Interestingly, the supramolecular organization of both Pcs was not observed in solution which was confirmed by optical absorption measurements. This result showed that the morphology of self-organization on the surface strongly depends on the features of the substrate, the chemical structure of the molecule, and molecule-to-molecule as well as molecule-to-surface interactions. Indeed, two different types of the self-organization, namely closed-packed arrays and properly ordered molecular wires were observed with symmetrical and unsymmetrical Zn(II)Pcs, respectively, on the HOPG surface. According to these results we can assume that the both intermolecular π–π and metal-ion coordination between two unsymmetrically substituted Pc units (**1**) are the driving force for the formation of nano-wire structures, whereas strong π–π interactions in the case of symmetric Zn(II)Pc **2** deposited on the HOPG surface facilitate the formation of closed-packed array. Although the results are still preliminary, further detailed investigations are necessary to better understand the supramolecular organization of these Pcs in different solvents and substrates. The research directed on these lines are undergoing in our group.

Acknowledgements

This work has been supported by Mersin University (BAP-FBE ESMB (SGC) 2014-2 YL). SGC thanks The Scientific and Technological Research Council of Turkey (TUBITAK) (grant no. 112T565) for financial support.

REFERENCES

1. (a) Barth JV, Costantini G and Kern K. *Nature* 2005; **437**: 671–679. (b) Yamamoto Y, Fukushima T, Suna Y, Ishii N, Saeki A, Seki S, Tagawa S, Taniguchi M, Kawai T and Aida T. *Science* 2006; **314**: 1761–1764. (c) Hoeben FJM, Jonkheijm P, Meijer EW and Schenning APHJ. *Chem. Rev.* 2005; **105**: 1491–1546. (d) Elemans JAAW, van Hameren R, Nolte RJM and Rowan AE. *Adv. Mater.* 2006; **18**: 1251–1266.
2. (a) Dimitrakopoulos CD and Malenfant PRL. *Adv. Mater*. 2002; **14**: 99. (b) Otsuki J. *Coord. Chem. Rev.* 2010; **254**: 2311–2341.
3. (a) Claessens CG, Uwe H and Torres T. *The Chemical Record.* 2008; **8**: 75–97. (b) de la Torre G, Claessens CG and Torres T. 2007; *Chem. Commun*. 2000. (c) de la Torre G, Bottari G, Sekita M, Hausmann A, Guldi DM and Torres T. *Chem. Soc. Rev.* 2013; **42**: 8049–8105.
4. (a) Rio Y, Rodriguez-Morgade MS and Torres T. *Org. Biomol. Chem.* 2008; **6**: 1877–1894. (b) Mack J and Kobayashi N. *Chem. Rev.* 2011; **111**: 281–321.
5. (a) de la Torre, Bottari G and Torres T. *Struct. Bond.* 2010; **135**: 1–44. (b) Bottari G, Suanzes JA, Trukhina O and Torres T. *J. Phys. Chem. Lett.* 2011; **2**: 905–913. (b) Guldi DM, Gouloumis A, Vázquez P, Torres T, Georgakilas V and Prato M. *J. Am. Chem. Soc.* 2005; **127**: 5811–5813. (c) Martínez-Díaz MV and Bottari G. *J. Porphyrins Phthalocyanines* 2009; **13**: 471–480. (d) Liu JY, Lo PC and Ng KPD. *Struct. Bond.* 2010; **135**: 169–210. (e) Bottari G, Trukhina O, Ince M and Torres T. *Coord. Chem. Rev.* 2012; **256**: 2453–2477.
6. (a) Hayashi H, Nihashi W, Umeyama T, Matano Y, Seki S, Shimizu Y and Imahori H. *J. Am. Chem. Soc*. 2011; **133**: 10736. (b) Ban K, Nishizawa K, Ohta K, van de Craats AM, Warman JM, Yamamoto I and Shirai H. *J. Mater. Chem.* 2001; **11**: 321–331. (c) Ince M, Martínez-Díaz MV, Barberá J and Torres T. *J. Mater. Chem*. 2011; **21**: 1531–1536.
7. Gómez-Segura J, Díez-Pérez I, Ishikawa N, Nakano M, Veciana J and Ruiz-Molina D. *Chem. Commun.* 2006; 2866–2868.
8. Liu Y, Lei S, Yin S, Xu S, Zheng Q, Zeng Q, Wang C, Wan L and Bai C. *J. Phys. Chem. B* 2002; **106**: 12569–12574.
9. Bottari G, Olea D, Gómez-Navarro C, Zamora F, Gómez-Herrero J and Torres T. *Angew. Chem. Int. Ed*. 2008; **47**: 2026–2031.
10. Sleven J, Görller-Walrand C and Binnemans K. *Mater. Sci. Eng. C* 2001; **18**: 229–238.
11. Shoji S, Hashishin T and Tamiaki H. *Chem. Eur. J*. 2012; **18**: 13331–13341.